SANDIA REPORT
SAND2008-7084
Unlimited Release
Printed October 2008

FY2008 Report on GADRAS Radiation Transport Methods

John Mattingly, Dean J. Mitchell, Lee T. Harding, Eric S. Varley, and Nathan R. Hilton

Prepared by
Sandia National Laboratories
Albuquerque, New Mexico 87185 and Livermore, California 94550

Sandia is a multiprogram laboratory operated by Sandia Corporation,
a Lockheed Martin Company, for the United States Department of Energy's
National Nuclear Security Administration under Contract DE-AC04-94AL85000.

Issued by Sandia National Laboratories, operated for the United States Department of Energy by Sandia Corporation.

Available to DOE and DOE contractors from
U.S. Department of Energy
Office of Scientific and Technical Information
P.O. Box 62
Oak Ridge, TN 37831

Telephone: (865) 576-8401
Facsimile: (865) 576-5728
E-Mail: reports@adonis.osti.gov
Online ordering: http://www.osti.gov/bridge

Available to the public from
U.S. Department of Commerce
National Technical Information Service
5285 Port Royal Rd.
Springfield, VA 22161

Telephone: (800) 553-6847
Facsimile: (703) 605-6900
E-Mail: orders@ntis.fedworld.gov
Online order: http://www.ntis.gov/help/ordermethods.asp?loc=7-4-0#online

SAND2008-7084
Unlimited Release
Printed October 2008

FY2008 Report on GADRAS Radiation Transport Methods

John Mattingly, Dean J. Mitchell, Lee T. Harding, and Eric S. Varley
Contraband Detection Department

Nathan R. Hilton
Radiation and Nuclear Detection Systems

Sandia National Laboratories
P.O. Box 5800
Albuquerque, New Mexico 87185-0791

Abstract

The primary function of the Gamma Detector Response and Analysis Software (GADRAS) is the solution of inverse radiation transport problems, by which the configuration of an unknown radiation source is inferred from one or more measured radiation signatures. GADRAS was originally developed for the analysis of gamma spectrometry measurements. During fiscal years 2007 and 2008, GADRAS was augmented to implement the simultaneous analysis of neutron multiplicity measurements. This report describes the radiation transport methods developed to implement this new capability.

This work was performed at the direction of the National Nuclear Security Administration's Office of Nonproliferation Research and Development. It was executed as an element of the Proliferation Detection Program's Simulation, Algorithm, and Modeling element.

Acronyms

BNL	Brookhaven National Laboratory
CSD	Continuous Slowing-Down
DU	depleted uranium
ENSDF	Evaluated Nuclear Structure Data Files
GADRAS	Gamma Detector Response and Analysis Software
HEU	highly enriched uranium
LANL	Los Alamos National Laboratory
LLNL	Lawrence Livermore National Laboratory
NA-22	Office of Nonproliferation Research and Development
NNDC	National Nuclear Data Center
NNSA	National Nuclear Security Administration
ODE	ordinary differential equation
ONEDANT	One-dimensional diffusion accelerated neutral particle transport
ORNL	Oak Ridge National Laboratory
PARTISN	Parallel time-dependent S_N
PDP	Proliferation Detection Program
RADSAT	Radiation Scenario Analysis Toolkit
RSICC	Radiation Safety Information Computational Center
SAM	Simulation, Algorithms, and Modeling
SNL	Sandia National Laboratories
SNM	special nuclear material
ToRI	Table of Radioactive Isotopes
URI	uniform resource identifier
XML	Extensible Markup Language

Contents

Figures

Tables

1 Introduction

During fiscal years 2007 and 2008, Sandia National Laboratories (SNL) was tasked by the National Nuclear Security Administration's (NNSA) Office of Nonproliferation Research and Development (NA-22) to develop and test new radiation transport methods and integrate them in GADRAS. This project was overseen by the Simulation, Algorithms, and Modeling (SAM) program management within NA-22's Proliferation Detection Program (PDP).

More specifically, SNL was tasked to

- Develop methods to analyze neutron multiplicity measurements and integrate them into GADRAS.
- Optimize the performance of the GADRAS radiation transport engine.
- Develop and implement improvements to neutron detector response models implemented in GADRAS.

The development of methods to rapidly and accurately compute neutron multiplicity metrics using deterministic transport was the primary enabling objective of the project. Achieving this objective has made it possible to integrate the analysis of neutron multiplicity measurements into GADRAS.

In order to achieve that primary objective, it was necessary to rebuild the majority of the GADRAS radiation transport engine. In addition to implementing procedures to calculate neutron multiplicity metrics from deterministic transport, we developed a new framework that is (1) more readily extensible to the computation of other measurable quantities, (2) constructed of modular components that can be reused by other developers for different applications, and (3) better optimized in terms of its computational performance.

Finally, in order to accurately model the response of neutron multiplicity counters, it was necessary to (1) improve existing models of those detectors' response characteristics and (2) develop methods to account for the effects of the measurement environment on those same response characteristics.

Developments to accomplish each of these tasks are described in this report following a brief background discussion of inverse radiation transport and GADRAS.

2 Inverse Radiation Transport and GADRAS

Radiation transport and detector response modeling have grown to substantial maturity, so that it is now possible to accurately predict the response of a variety of radiation sensors to arbitrary but *known* sources. However, in many applications, particularly those that support the nonproliferation mission, the *inverse* problem is more directly relevant. That problem is to estimate the configuration of an *unknown* radiation source given one or more of its measured signatures. This is the problem of inverse radiation transport.

The original and principal purpose of GADRAS is to solve the inverse radiation transport problem. The code is designed to enable an analyst to infer the configuration of an unknown radiation source from its measured radiation signatures.

The practical solution of inverse transport problems imposes three basic requirements:

1. to be solvable; the problem must be constrained to have a limited number of degrees of freedom,
2. the transport and detector response calculations must be accurate to avoid biasing the solution, and
3. transport calculations must execute quickly so that iteration towards a solution converges in a reasonable time.

GADRAS is composed of three basic components that work together to solve the inverse transport problem:

1. a radiation transport framework,
2. one or more detector response models, and
3. a nonlinear optimization procedure.

These three components are implemented to meet the preceding requirements for the practical solution of inverse transport problems.

- ***Radiation Transport***: GADRAS combines (1) S_N deterministic transport to solve for the energy group averaged electron, neutron, and photon flux and leakage current with (2) photon ray-tracing to solve for the discrete energy photon leakage current. These deterministic methods were chosen in favor of Monte Carlo methods for their computational speed. The primary function of the radiation transport framework is to estimate the spectral (and for some detectors, temporal) distribution of radiation incident on detectors measuring the modeled source.
- ***Detector Response Model***: GADRAS employs a point model of detector response functions. Response models are implemented for gamma spectrometers, gross neutron counters, and neutron multiplicity counters. These response functions model the spectral response of the detector(s) to incident radiation. In order to model the response of neutron multiplicity counters, the detector response model also accounts for the temporal response characteristics of the detector.
- ***Nonlinear Minimization***: GADRAS employs a modification of the Levenberg-Marquardt nonlinear minimization procedure. This procedure seeks the transport model parameters that minimize the error between the computed and measured radiation signatures. A chi-squared metric, which is the variance-weighted sum of square errors between the model and the measurement, is used as the metric to be minimized by the optimization procedure. Because most gamma spectrometry instruments acquire a single spectrum that is integrated over the sensor's entire spatial field of view, problems are constrained to have a single spatial dimension, i.e., the source is modeled as a series of one-dimensional material layers. The model parameters optimized by the nonlinear minimization procedure are the thicknesses of individual layers.

An inverse transport problem (refer to Figure 1) is solved by first hypothesizing a model for the unknown radiation source. Development of this initial model is assisted by several automated analysis techniques that are also implemented in GADRAS but are beyond the scope of this report. The radiation transport framework calculates the neutron and photon fields incident on the detectors, and the detector response models transform those fields into predicted detector responses. These predicted responses are compared to the measured responses, and the nonlinear optimization procedure iteratively modifies the parameters of the initial model until the predicted responses match the measured responses.

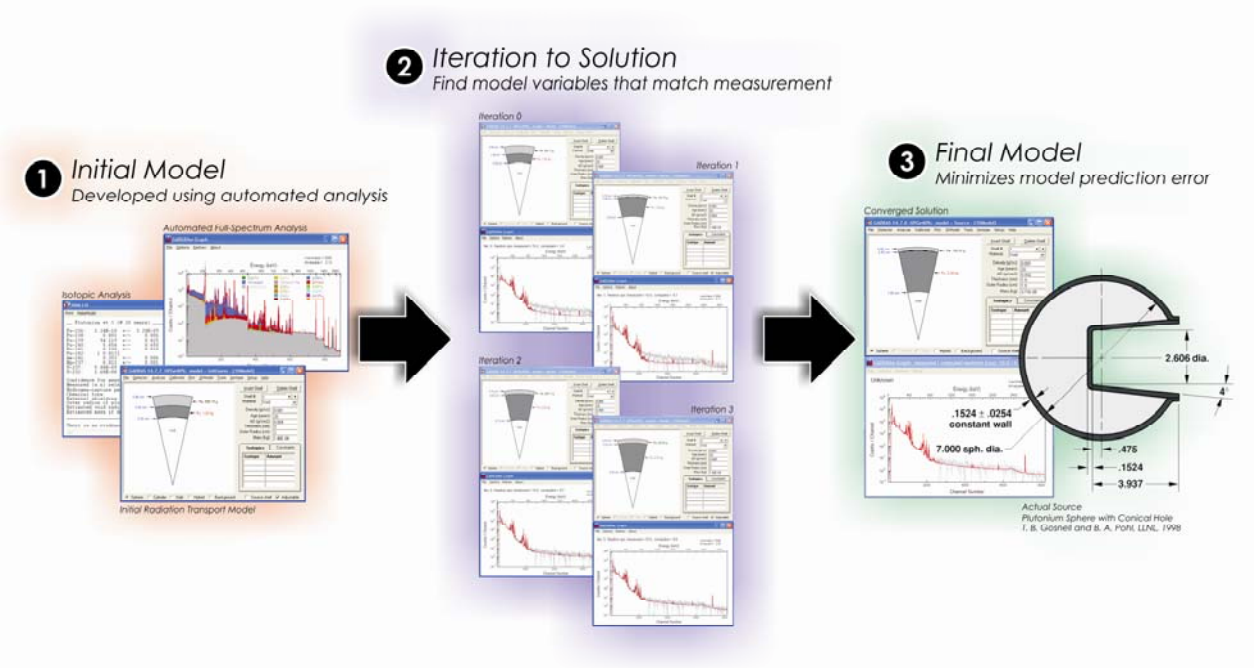

Figure 1. Iterative solution of an inverse transport problem. The measurement analyzed was acquired from an unclassified, 2.4 kg of weapons-grade plutonium metal sphere. [Gosnell and Pohl]

In general, inverse transport problems do not possess unique solutions. However, by simultaneously analyzing multiple complementary measured signatures, the problem can be constrained to be solvable in most cases. As its name implies, GADRAS was originally developed to solve the inverse problem via analysis of gamma spectrometric measurements. However, due to the self-shielding properties of most special nuclear materials, the solutions to many inverse problems are poorly constrained when based only upon the analysis of gamma spectral measurements.

By simultaneously analyzing observables derived from the neutron field, e.g., the count rate measured by a neutron detector, many such challenging problems can be better constrained. However, a measured neutron count rate conveys relatively limited information regarding the neutron field. Consequently, under the SAM program's direction, SNL has modified the radiation transport engine and neutron detector response models implemented in GADRAS to predict the response of neutron

multiplicity detectors. These detectors acquire measurements that help to constrain the neutron source intensity, neutron multiplication, and neutron lifetime. Simultaneous analysis of a measured gamma spectrometer and neutron multiplicity counter-response constrains most inverse problems fairly tightly.

In order to implement these new capabilities, the radiation transport framework implemented in GADRAS has undergone numerous changes. These changes, and the new capabilities they imbue, are described in the subsequent section.

3 Radiation Transport Framework

The primary function of the GADRAS radiation transport framework is the synthesis of a mixed neutron and gamma radiation field from a simple model of radiating and shielding materials. Users can construct a one-dimensional model of a heterogeneous radiation source consisting of layers of radioactive and stable materials. The transport framework constructs from that model several transport problems including

- ***Electron transport problem***: the electron transport problem is solved to estimate the generation of electron-bremsstrahlung photons.
- ***Alpha transport problem***: the alpha transport problem is solved to estimate the generation of neutrons and gammas from nuclear alpha capture interactions.
- ***Neutron transport problem***: the neutron transport problem is solved to estimate the neutron field incident on a gross neutron counter, neutron multiplicity counter, or a gamma spectrometer. The neutron field is used to estimate the count rate in a gross neutron counter, the mean and variance of the neutron counting distribution measured by a neutron multiplicity counter, and/or the amplitude of (n, γ) and (n, n′) photopeaks due to neutron interactions in a gamma spectrometer. The solution is also used to estimate the generation of gammas via induced fission, neutron capture, and neutron inelastic scatter.
- ***Photon transport problem***: the photon transport problem is solved to estimate the photon field incident on a gamma spectrometer. The solution is used to estimate the Compton continuum measured by a gamma spectrometer.
- ***Photon ray/trace problem***: the photon ray/trace problem is solved to estimate the field of uncollided photons incident on a gamma spectrometer. The uncollided photon field is used to synthesize gamma spectrum photopeaks to arbitrary precision.

The transport framework invokes numerical solvers for each of the preceding transport problems to solve the overall coupled electron/neutron/photon transport problem.

Subsequent sections describe the components of the radiation transport framework.

3.1 Nuclide Database

Prior to 2008, GADRAS employed a database of radionuclide gamma emissions based primarily on the information published in the Table of Radioactive Isotopes (ToRI) [Firestone Richard B. et al.] The GADRAS database included 179 of the most frequently encountered natural, industrial, medical, fission product, and SNM

radionuclides. The gamma emission spectra of several nuclides, most notably SNM nuclides, were corrected to match benchmark experiments.

The new radiation transport framework employs a nuclide database derived from the Evaluated Nuclear Structure Data Files (ENSDF) maintained and distributed by the National Nuclear Data Center (NNDC) at Brookhaven National Laboratory (BNL). Most other published nuclide tables, including the ToRI, ultimately derive from the ENSDF.

The nuclide database is used to model the composition of radioactive materials accounting for their decay over time by solving the branching Bateman decay equations, which is done in real time as the radiation transport sequence executes. The database is also used to compute the alpha, beta, positron, electron capture, and gamma spectra necessary to model the source terms associated with radioactive materials.

The new database currently tabulates the decay and emission properties of over 1100 different nuclides, which is an order-of-magnitude increase over the database distributed with GADRAS just two years ago. It also incorporates several corrections to the gamma spectra of uranium-235, uranium-238, plutonium-239, plutonium-240, and americium-241 that are not included in the ENSDF as distributed by the NNDC. The corrections were developed to match several benchmark measurements of bulk quantities of SNM. [Varley and Mattingly]

In general, the benchmark measurements do not meet the criteria for publication into the Nuclear Datasheets, which is required to incorporate the corrections in the ENSDF. However, we may publish our nuclide database, which is formatted in XML, through a website that permits submission of peer-reviewed corrections. We have discussed this possibility with the larger analyst community, and there is significant interest in establishing a committee involving analysts at SNL, Los Alamos National Laboratory (LANL), and Lawrence Livermore National Laboratory (LLNL) to review corrections and amendments to the database and jointly manage its publication.

An example of a screen from the XML nuclide database is shown in Figure 2.

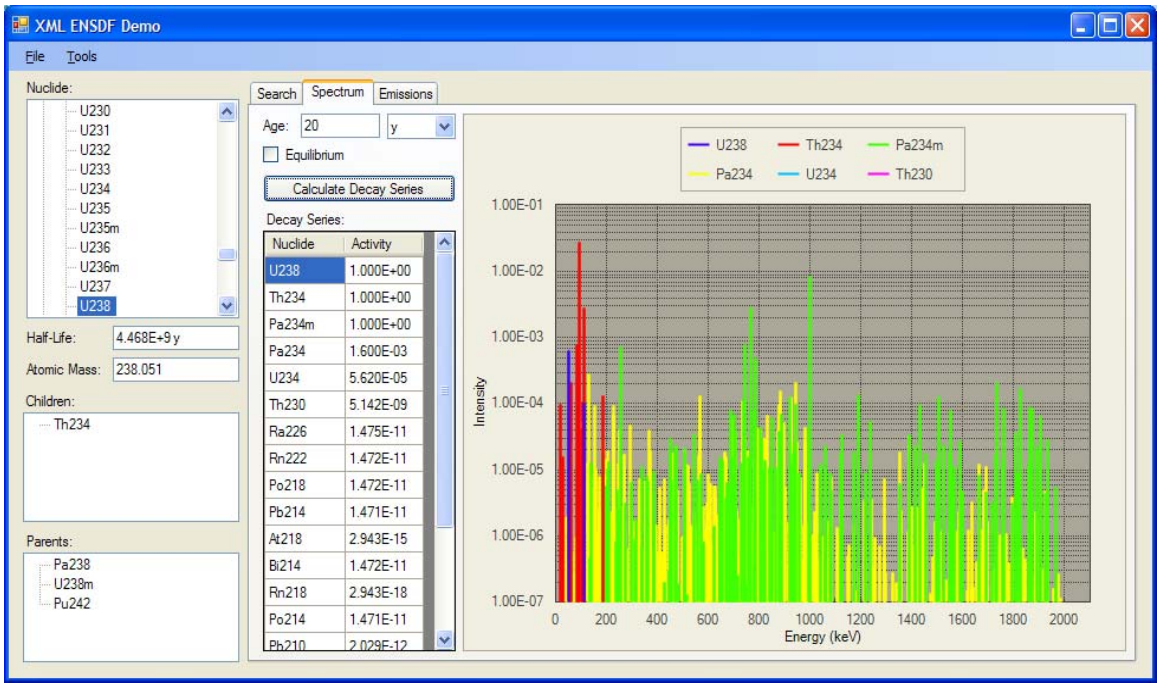

Figure 2. Uranium-238 decay series and gamma emissions after 20 years aging

3.2 Electron Transport

If the transport model contains beta-emitting materials, the transport framework will execute an electron transport calculation to estimate the production of photons via electron-induced bremsstrahlung radiation. Bremsstrahlung photons result when free electrons (i.e., beta particles emitted by neutron-rich radionuclides) decelerate under the influence of orbital electrons due to Coulombic repulsion. The distribution of brems-strahlung photons is continuous over energy up to the maximum beta energy (i.e., the beta endpoint energy), so they create a continuous contribution to the photon leakage current and hence to the spectrum measured by a gamma spectrometer. Brems-strahlung is a dominant component of the photon leakage spectrum of bulk uranium-238, and for some radionuclides such as strontium-90, it is the only source of photon production. Consequently, accurate synthesis of the gamma spectrum requires computation of electron-bremsstrahlung photon production.

The majority of the components used for electron transport were previously developed and tested in 2005. [Mattingly] They were integrated in 2008 into the coupled electron/ neutron/photon transport framework that is now distributed with GADRAS.

3.2.1 Electron Source Terms

Electron source terms are computed using Fermi's relativistic model of the beta spectrum for allowed beta transitions. [Evans] We have not implemented separate models for unallowed beta transitions, primarily because no generally applicable models exist. The composite beta spectrum for a radioactive material is constructed using the beta endpoint energies and intensities supplied by the nuclide database.

3.2.2 Electron Transport Cross-Sections

Electron transport cross-sections were generated using CEPXS, a multigroup, Legendre-coupled electron-positron-photon cross-section generating code developed by SNL and distributed by the Radiation Safety Information Computational Center [RSICC] at Oak Ridge National Laboratory (ORNL). [Lorence, et al. October 1989] The cross-sections used in the electron transport sequence include all the elements between hydrogen and americium.

3.2.3 Electron Transport Solver

The Boltzmann-Continuous Slowing-Down (CSD) equation for electrons is solved for the electron flux using the one-dimensional discrete ordinates code ONEDANT-LD (a.k.a., ONELD) developed by SNL and distributed by RSICC. [Lorence, et al. September 1989] ONELD is a modification of the one-dimensional discrete ordinates solver ONEDANT[1], originally developed by LANL [Alcouffe et al. 1995]. ONELD uses a linear-discontinuous spatial differencing approximation to represent the gradient in the electron flux, which can exhibit sharp discontinuities at material boundaries.

3.2.4 Electron-Bremsstrahlung Photon Source Generation

Electron-induced bremsstrahlung photon radiation is generated by folding the electron flux with electron-bremsstrahlung cross-sections extracted from the EL03 electron transport library that is distributed with MCNP [Adams]. The position- and energy-dependent distribution of bremsstrahlung photons is used as a source term in the final photon transport step.

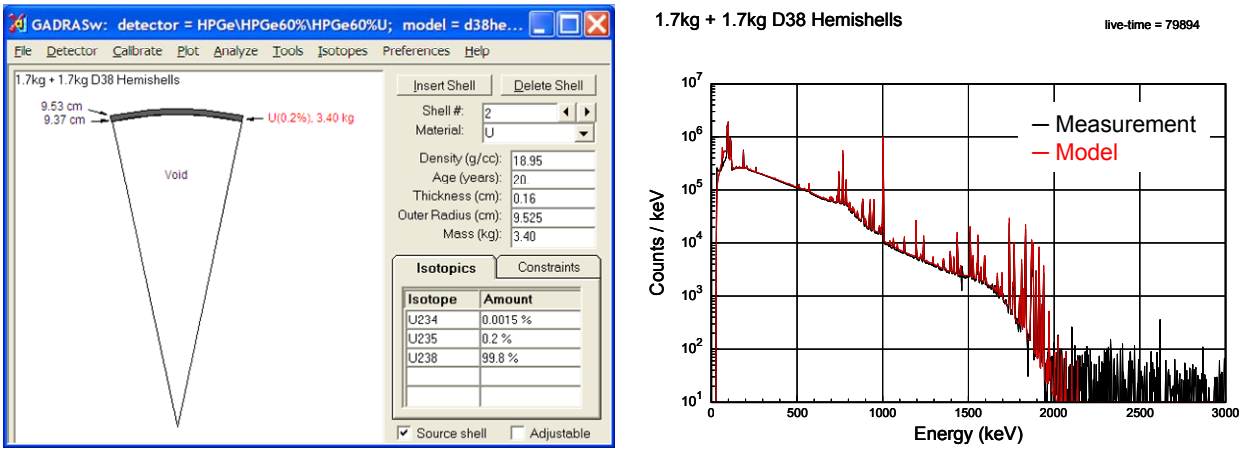

Figure 3. Comparison of a measurement of a depleted uranium shell to transport calculation. The majority of the continuum evident in the gamma spectrum results from electron-bremsstrahlung

[1] One-dimensional diffusion accelerated neutral particle transport.

3.3 Neutron Transport

The transport framework will execute a neutron transport calculation if the transport model meets one or more of the following conditions:

- The model contains spontaneous fission materials.
- The model contains materials that mix alpha-emitting radionuclides and light nuclides (atomic number ≤ 17).
- The model contains an interface between an alpha-emitting material and a material containing light nuclides.

In the first case, the model contains a source of spontaneous fission neutrons. In the latter two cases, the model contains a source of neutrons resulting from (α, n) reactions. Spontaneous fission and (α, n) reactions are the dominant spontaneous neutron production processes in passive measurements. In an (α, n) reaction, an alpha particle is captured by a nucleus, and the resulting product nucleus decays from its excited state by emission of a neutron (and sometimes other things, including protons and photons). Alpha particles spontaneously emitted during the alpha decay of proton-rich nuclei are generally only energetic enough to penetrate the Coulombic barrier of lighter nuclei (e.g., chlorine isotopes and below).

The neutron transport calculation is used to estimate the following:

- The response of a gross neutron counter (i.e., a proportional counter).
- The response of a gamma spectrometer to (n, γ) and (n, n′) reactions in the detector's sensitive material.
- The response of a neutron multiplicity counter. There are numerous potential metrics of a multiplicity counter's response. The current implementation estimates the mean and variance of the measured counting distribution versus counting time.
- The production of secondary photon source terms due to induced fission, capture, and inelastic scatter.

3.3.1 Neutron Source Terms

Neutron source terms from spontaneous fission and (α, n) reactions are generated using the SOURCES-4C code developed by LANL and distributed by RSICC [Wilson, et al.]. SOURCES-4C uses the Watt model to compute the spontaneous fission neutron spectrum of 30 different nuclides. The code uses simplified alpha transport to compute the neutron spectrum resulting from (α, n) reactions from 48 different alpha-emitting nuclides interacting with 16 different light target nuclides. SOURCES-4C can compute the neutron spectrum from (α, n) reactions in homogeneous materials and across material interfaces. The transport framework uses the Terrell model to calculate the distribution of the number of neutrons per spontaneous fission [Terrell].

Prior to 2008, GADRAS implemented models of spontaneous fission neutron spectra for only the most frequently encountered sources. It used a collection of lookup tables to model the (α, n) neutron spectra for only a handful of alpha emitters, and light target nuclides were restricted to beryllium, lithium, and oxygen isotopes. Consequently, the

integration of SOURCES-4C into the transport framework represents an order-of-magnitude improvement in GADRAS's ability to model neutron-emitting radioactive materials.

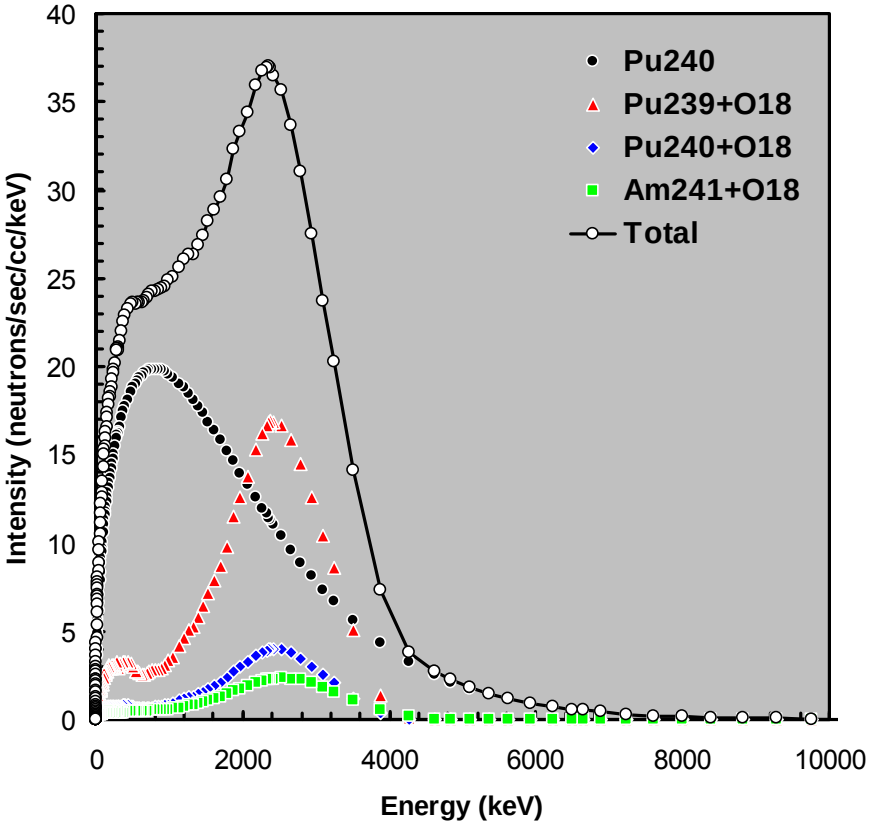

Figure 4. Neutron source terms computed by SOURCES-4C for 1 kg of weapons-grade plutonium oxide

3.3.2 Neutron Transport Cross-Sections

Several alternative neutron cross-section libraries were evaluated for use in the transport framework. Ultimately, the choice of cross-section library is dictated by the balance between computational accuracy and speed.

In practice, multigroup neutron cross-sections are often developed for problem-specific applications. This practice permits an energy group structure and weighting function specific to a particular class of problem to be chosen *a priori*. The group structure and weighting function are then used to generate a library that is accurate for its specific problem class and enables very rapid solution of the transport equation. The problem-specific library is generated by collapsing a problem-independent library with a fine group structure onto a much coarser group structure.

In order to use a problem-specific library, the problem's spectral characteristics must be known in advance. Unfortunately, the human reasoning used to classify a particular

problem's spectral properties is difficult to automate without first solving the transport equation.

Alternatively, a problem-independent library can be employed. Generally speaking, problem-independent libraries employ a fine energy group structure that is accurate for a very wide range of problem classes. However, that fine structure tends to slow the solution of the transport equation. As their name implies, little or no *a priori* knowledge of the problem's spectral characteristics is required.

We chose to use a problem-independent neutron cross-section library in the GADRAS transport framework. Although the on-demand generation of problem-specific libraries is relatively fast, automation of that process still requires some mechanism to estimate the neutron spectrum so that a weighting function and coarse group structure can be chosen. For three-dimensional problems, those decisions are generally made by solving a one-dimensional approximation to the full problem using a problem-independent library (i.e., using a coarse spatial approximation with a fine spectral approximation). However, since the GADRAS transport framework is built around the rapid solution of one-dimensional problems, that procedure will yield no performance enhancement. Instead, we devoted some effort to developing a cross-section library that reasonably balanced computational accuracy and speed.

During the development and testing of the new transport framework, three alternative neutron cross-section libraries were evaluated.

- ***SNAPPLE library***: The SNAPPLE library was generated for SNL by ORNL in 2004 as an extension of an earlier custom-built library [Alpan and Dunn]. The SNAPPLE library has 47 neutron energy groups, with only three broad groups that encompass most thermal energies. The weighting function used to compute the group-averaged cross-sections is a generic Watt fission spectrum. Furthermore, the SNAPPLE scatter matrices do not contain upscatter elements, which account for the tendency of thermal neutrons to sometimes emerge from a scatter reaction with more kinetic energy than they originally had. Because the SNAPPLE library uses a relatively small number of energy groups and lacks upscatter, it enables extremely fast solution of the transport equation. However, the library's coarse thermal energy group structure in conjunction with the weighting function and the absence of upscatter make the library inaccurate for problems exhibiting a highly thermalized neutron population. This potential for inaccuracy has been observed for some neutron gross counting calculations in the past, though the errors observed were too slight to prompt further investigation. However, when we began testing new methods to calculate neutron multiplicity counting metrics, that deficiency became clearly evident [Mattingly and Varley]. The SNAPPLE library is not generally usable for the computation of neutron multiplicity counter responses; it exhibits enormous errors relative to measurements of highly thermalized systems.
- ***VITAMIN-B6 library***: The VITAMIN-B6 library is a problem-independent library developed by ORNL and distributed by RSICC [J. E. White et al.]. It uses a fairly fine group structure that has 199 neutron energy groups; the thermal energy range is covered by 35 groups. The weighting function is a general purpose spectrum that is

composed of a Maxwellian spectrum at thermal energies, a 1/E slowing-down spectrum over intermediate energies, and an uncollided Watt fission spectrum at high energies. Most importantly, the library's scatter matrices contain upscatter elements for the 35 thermal energy groups. Consequently, the library enables accurate solution of the transport equation for a wide range of problems including those exhibiting a highly thermalized neutron population. However, the large number of energy groups substantially slows solution of the transport equation. Consequently, though the VITAMIN-B6 library is generally usable for computation of neutron multiplicity counter responses, it induces unacceptably long computational times.

- ***Kynea3 library***: The Kynea3 cross-section library was developed for this project during 2007 and 2008 to obtain the speed of the SNAPPLE library while preserving the accuracy of the VITAMIN-B6 library [Varley and Mattingly June 2008]. The Kynea3 library is a hybrid between the SNAPPLE and VITAMIN-B6 libraries. It was generated by collapsing the VITAMIN-B6 library onto a coarser group structure using the SCALE system maintained by ORNL and distributed by RSICC [SCALE]. Kynea3 uses the VITAMIN-B6 weighting function, the fine group structure and upscatter elements of the 35 low-energy VITAMIN-B6 groups, and the coarser group structure of the 44 high-energy SNAPPLE groups.

The next two figures compare the results obtained from the three libraries.

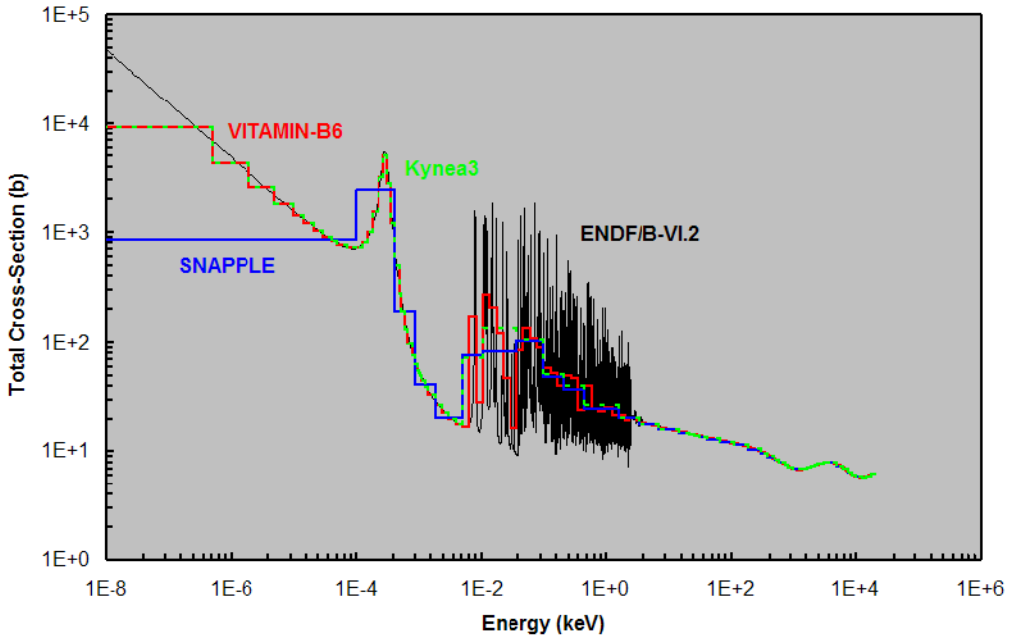

Figure 5. Comparison of plutonium-239 total cross-section for point-wise ENDF/B-VI.2, SNAPPLE, VITAMIN-B6, and Kynea3 libraries

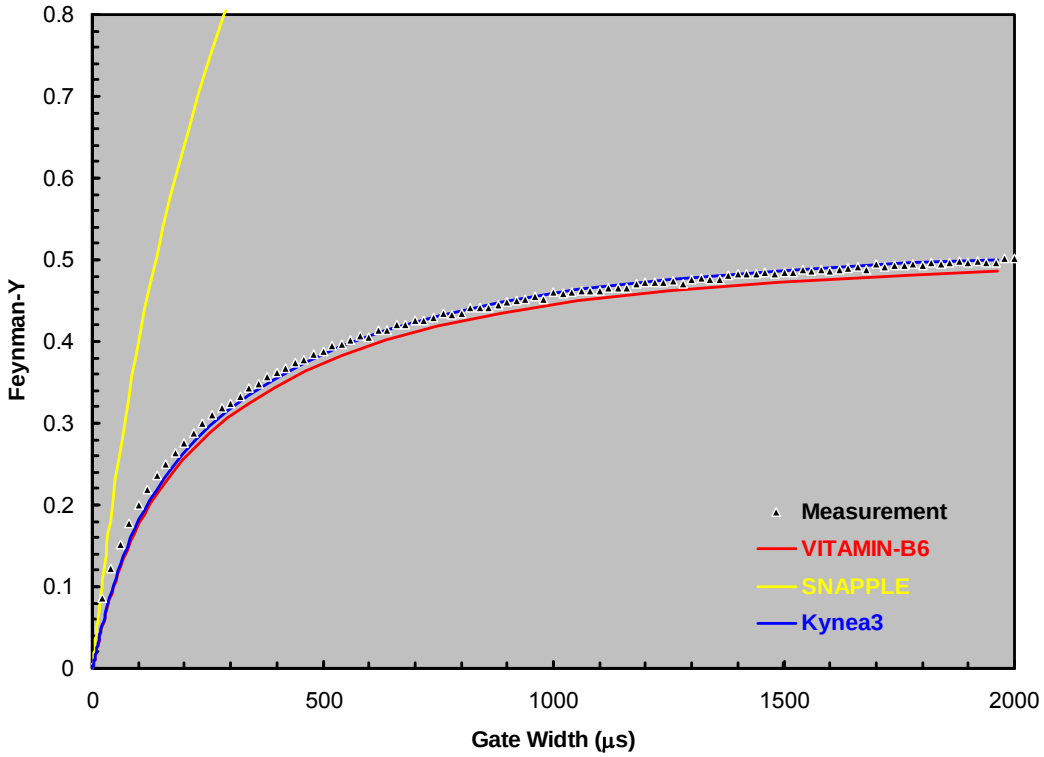

Figure 6. Comparison of neutron multiplicity measurement to calculations using SNAPPLE, VITAMIN-B6, and Kynea3 cross-section libraries. The source was an unclassified 4.4-kg sphere of weapons-grade plutonium metal reflected by six inches of polyethylene [Valentine 2006].

Most calculations using the Kynea3 library execute in one-third to one-quarter of the computational time used by the VITAMIN-B6 library (see Table 1). Calculations using the Kynea3 library are still slightly slower than those using the SNAPPLE library. However, we were able to modify other parts of the full coupled transport sequence to reduce the overall computational time by 25% or more. Moreover, in every test case, the Kynea3 library produced results that were as accurate as those obtained using the VITAMIN-B6 library. The Kynea3 library is now distributed with GADRAS.[2] It contains neutron cross-sections for 145 different nuclides and elements.

[2] The Kynea3 library has also been shared with Pacific Northwest National Laboratory (PNNL) to support the RADSAT (Radiation Scenario Analysis Toolkit) program.

Table 1. Comparison of computational times to synthesize neutron multiplicity detector response using SNAPPLE, VITAMIN-B6, and Kynea3 cross-section libraries. Cases shown are for an unclassified 4.4-kg sphere reflected by polyethylene shells of varying thickness.

Library	Poly Thickness (in)	Time (sec)			
		Forward	Adjoint	Dynamic	Total
SNAPPLE (47 group)	0	0.2	0.4	1.5	2.1
	0.5	0.3	0.3	2.9	3.6
	1	0.3	0.3	3.5	4.1
	1.5	0.4	0.3	4.2	4.9
	3	0.4	0.4	5.9	6.7
	6	0.4	0.8	6.7	8.0
VITAMIN-B6 (199 group)	0	2.1	2.4	8.0	12.5
	0.5	2.7	3.6	21.9	28.2
	1	3.0	3.1	28.6	34.8
	1.5	3.4	4.2	34.6	42.2
	3	4.2	6.1	43.2	53.5
	6	6.4	5.7	47.0	59.1
Kynea3 (79 group)	0	0.4	0.6	2.5	3.5
	0.5	0.7	0.8	6.0	7.6
	1	0.7	0.7	8.0	9.5
	1.5	0.8	0.9	9.3	11.0
	3	1.1	1.4	11.9	14.4
	6	1.8	1.5	13.0	16.3

3.3.3 Neutron Transport Solver

The new transport framework uses PARTISN[3] to solve the Boltzmann neutron transport equation. PARTISN is designed to solve the full time-dependent forward and adjoint Boltzmann transport equation in three spatial dimensions using discrete ordinates [Alcouffe et al. 2005]. As a component of the GADRAS transport framework, it is used to solve the static (time-independent) forward and adjoint transport equation and the dynamic (time-dependent) forward transport equation in one dimension. PARTISN was developed and is maintained by LANL; it is distributed by RSICC.

The neutron transport solution is the most complicated step in the overall transport sequence because one to three calculations are required depending on the neutron detector response that will be computed. For gross neutron counters, only a single static forward transport solution is required. For neutron multiplicity counters, a static adjoint transport solution and a dynamic forward transport solution are also required.

[3] Parallel time-dependent S_N.

The three needed equations are:

- ***Forward solution***: The usual formulation of the time-independent transport equation is solved for the neutron flux and the leakage current. The source terms for this problem are dictated by the spontaneous fission and (α, n) neutron emissions of the materials in the transport model, as previously discussed. The neutron flux is used to compute photon source terms arising from neutron interactions, and the leakage current is used to compute the neutron detector average count rate as well as the neutron response of the gamma spectrometer. The forward flux is also used to estimate the rate of neutron production via induced fission, which is used in conjunction with the adjoint flux to compute the variance in the neutron count rate. The distribution of the number of neutrons from induced fission is calculated using Zucker and Hölden's measurements for uranium-235, uranium-238, and plutonium-239 [Zucker and Holden]. We expect to extend these models to other fissile nuclides in the near future using the same method implemented by Valentine [2001] in MCNP-DSP.
- ***Adjoint solution***: The time-independent adjoint transport equation is solved for the adjoint flux. The solution to the adjoint formulation of the Boltzmann transport equation represents the importance of neutrons to the effect embodied in the adjoint source term. For example, if the adjoint source term is the fission cross-section, then the adjoint flux represents the likelihood that a neutron in a particular location in (time, position, energy, direction) phase space will induce a fission. The adjoint flux is effectively a weighting function that can be used in conjunction with the forward flux to compute an effect like the induced fission rate. For our application, the adjoint source term is the neutron detector efficiency. Consequently, the adjoint flux represents the likelihood that a neutron at a particular location in phase space will result in a count in the detector. This weighting function is used in conjunction with the forward flux to compute the variance in the neutron count rate, which is a metric (the second moment) of the distribution measured by neutron multiplicity counters. The variance can be used in conjunction with the mean (the average count rate) to constrain the neutron multiplication of the system.
- ***Dynamic forward solution***: The time-dependent forward transport equation is solved for the leakage current versus time. The source term for this problem is the normal forward source term with its amplitude instantaneously stepped from zero to its full value at the beginning of the calculation. Consequently, the solution represents the dynamic step response of the system. The time-dependent leakage is used to estimate the dynamic step response of the neutron multiplicity counter, which determines the evolution of the variance in the counting distribution with increasing counting time. The time-evolution of the variance can be used to constrain the neutron lifetime of the system.

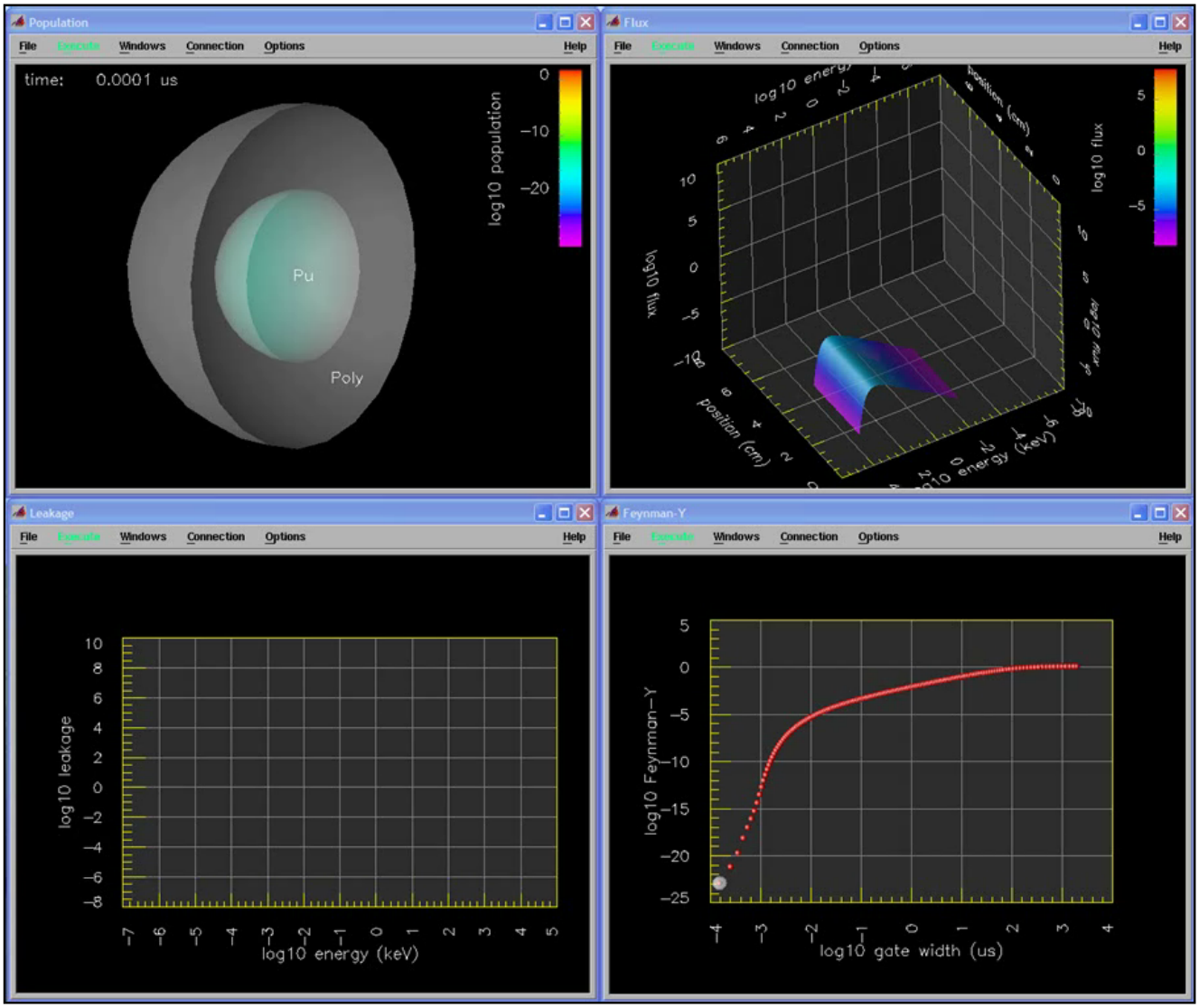

Figure 7. Dynamic calculation of a neutron multiplicity counter response (click on the image to play movie). The source shown is a plutonium sphere reflected by polyethylene.

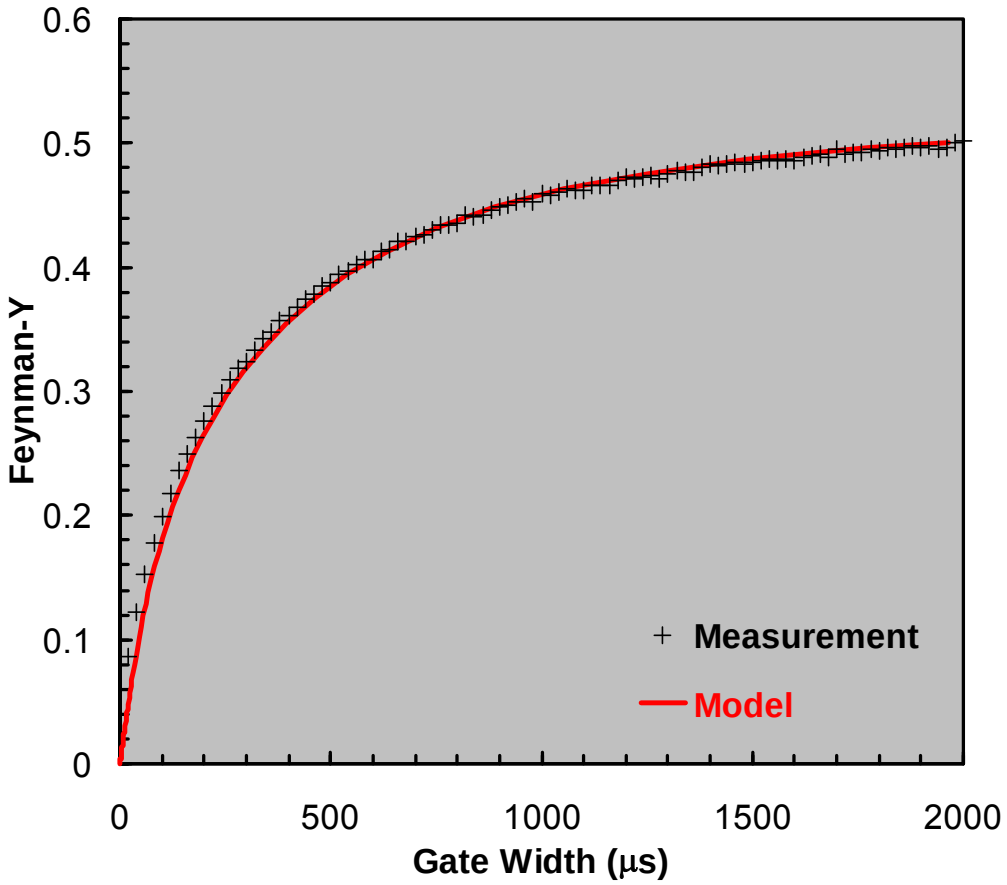

Figure 8. Comparison of measured and calculated neutron multiplicity counter response. The source was an unclassified 4.4-kg sphere of weapons-grade plutonium metal reflected by 6 inches of polyethylene.

3.3.4 Neutron-Induced Photon Source Generation

The neutron flux obtained by solving the forward transport problem is used to compute secondary photon production via induced fission and neutron capture and inelastic scatter, as described below:

- ***Induced fission gammas***: The induced fission rate is estimated by folding the neutron flux with the fission cross-section of fissionable materials in the transport model. The resulting induced fission rate is used to estimate the production of induced fission gammas. On average, each induced fission yields 7.7 prompt gammas and 6.8 delayed gammas, which are fairly typical for most fissionable nuclides. The fission gamma spectrum is computed using Maienschein's model [Peelle and Maienschein, Maienschein].
- ***Neutron capture and inelastic scatter gammas***: the neutron flux is folded with the neutron capture and inelastic scatter cross-sections of all the materials in the transport model. These cross-sections were extracted from the ENDF66 and ACTI

libraries distributed with MCNP [Monte Carlo Team]. Our (n, γ) database tabulates the neutron capture and inelastic scatter cross-sections of 76 different nuclides and elements for over 10,000 different gamma lines.

The secondary gamma production resulting from these reactions is used as an additional source term for the final photon transport step.

3.4 Photon Transport

The transport framework will execute a photon transport calculation if the model contains any primary (i.e., spontaneous) gamma sources or secondary (i.e., induced) gamma sources. The photon transport calculation is used to compute the leakage spectrum of photons, which is in turn used to estimate the gamma spectrometer's response.

The photon leakage spectrum is estimated in two computationally distinct steps. In the first step, the photon transport equation is numerically solved for the group-averaged leakage current, which includes both collided (scattered) and uncollided photons. In the second step, numerical ray-tracing is used to estimate the leakage of uncollided discrete-energy photons (gammas and x-rays). By computing the uncollided leakage using ray-tracing, photopeaks in a gamma spectrometer's response can be synthesized to arbitrary resolution.

3.4.1 Photon Source Terms

The photon transport step uses the following source terms:

- ***Nuclear decay gammas***: When unstable nuclei undergo spontaneous alpha decay, beta decay, or electron capture, the transmuted child nucleus is almost always in an excited state. The child nucleus generally decays through a cascade of energy levels via gamma emission. The energies and intensities of these gamma emissions are provided by the nuclide database, which contains over 35,000 nuclear decay gamma lines.
- ***Spontaneous fission gammas***: On average, 7.7 prompt and 6.8 delayed gammas are emitted following a spontaneous fission. The spontaneous fission gamma spectrum is calculated using the same model (Maienschein's) used for induced fission gammas.
- ***(α, n) gammas***: (α, n) reactions (in fact, virtually all alpha absorptions) generally leave the product nucleus in a highly excited state. Some of the most energetic gamma lines observed in gamma spectrometry measurements result from the decay of nuclei following an alpha absorption. Unfortunately, though the energies of these gammas are typically known very precisely, their intensities are relatively poorly known for many reactions. The current implementation of the transport framework includes the gamma spectra resulting from the most commonly encountered alpha absorption reactions with beryllium-9, nitrogen-14, oxygen-17, oxygen-18, and fluorine-19. LLNL has conducted a fairly extensive, but relatively undocumented, series of gamma spectrometry measurements on different (α, n) sources. We may attempt to incorporate that information in the future.

- ***Neutron-induced fission gammas***: Prompt and delayed gammas from induced fission are computed by folding the neutron flux with the fission cross-sections of the model materials. For more detail, refer to the preceding section on neutron-induced photon source generation.
- ***Neutron capture and inelastic scatter gammas***: gammas from neutron capture and inelastic scatter reactions are computed by folding the neutron flux with the (n, γ) cross-sections of the model materials. For more detail, refer to the preceding section on neutron-induced photon source generation.
- ***Electron-bremsstrahlung photons***: photons from bremsstrahlung are computed by folding the electron flux with the electron-bremsstrahlung cross-sections of the model materials. For more detail, refer to the preceding section on electron-bremsstrahlung photon source generation. Currently, the transport framework does not compute the photon source term resulting from positron-bremsstrahlung. We may incorporate positron transport in the near future.

3.4.2 Photon Transport Cross-Sections

Photon transport cross-sections were generated using GAMLEG-JR, a code developed by the Japanese Atomic Energy Research Institute (JAERI) and distributed by RSICC [Miyasaka and Minami]. GAMLEG-JR uses analytical models of the photoelectric absorption and pair-production cross-sections developed by the National Institute of Standards and Technology (NIST) and the Klein-Nishina scatter kernel to generate photon absorption and scatter cross-sections. The code analytically expands the Klein-Nishina scatter kernel in Legendre polynomials to represent its angular dependence, and it numerically integrates the absorption and scatter cross-sections over a user-specified energy group structure. The photon cross-section library currently distributed with GADRAS was generated in 2004. In the near future, we may replace it with a library generated using the same code (CEPXS) that we used to generate the electron cross-section library mainly to simplify maintenance of the transport framework.

3.4.3 Photon Transport Solver

Currently, the Boltzmann transport equation for photons is solved using the same solver ONELD that is used to solve the Boltzmann-CSD equation for electrons. Either ONELD or PARTISN can be used to solve the photon transport problem. However, the version of PARTISN solver currently integrated in the new transport framework does not implement linear discontinuous (LD) spatial differencing for one-dimensional problems. Consequently, PARTISN is relatively slower than ONELD, and since only the time-independent transport equation needs to be solved for photons, ONELD is used to solve that problem instead of PARTISN. We have acquired a more recent version of PARTISN from LANL; that newer version does implement LD spatial differencing in one dimension. We expect to replace the version of PARTISN currently distributed with the transport framework with the newer version in the near future. At that time, depending upon the computational speed of PARTISN vs. ONELD, we may choose to solve the photon transport problem using PARTISN.

The flux obtained from the solution to the photon transport problem is used to generate a fluorescence x-ray source term, which is subsequently used in the photon ray-tracing

step to include x-rays in the computed gamma spectrometer response. Fluorescence x-ray cross-sections were extracted from the Evaluated Photon Data Library (EPDL) developed by LLNL, and x-ray energies and intensities were extracted from the ToRI database [Cullen, et al.]. The x-ray database distributed with the transport framework tabulates over 1,600 X rays.

The continuum contribution resulting from x-ray scattering is not currently calculated because (1) it would require yet another solution to the transport equation, which is computationally expensive, and (2) most of the contribution of Compton-scattered X rays falls below the lower-level discrimination of typical gamma spectrometers.

3.5 Photon Ray-Tracing

Discrete-energy photon source terms result from three distinct processes:

- ***Nuclear decay***: The nuclear decay gamma source term is computed according to the radionuclides present in the model materials. This source term is spatially uniform over contiguous material regions.
- ***Nuclear alpha absorption***: Gammas arising from nuclear alpha absorption are modeled for the most commonly encountered target materials. This source term is spatially uniform over contiguous material regions. The source term also occurs at the boundary between alpha-emitting materials and materials containing light nuclides, where it is practically a surface source.
- ***Neutron capture and inelastic scatter***: Gammas resulting from neutron capture and inelastic scatter are calculated from the neutron flux folded with the (n, γ) cross-sections of the model materials. This source term varies with position within contiguous material regions due to the spatial variation in the neutron flux.

The uncollided leakage of these photons through the outer boundary of the transport model is estimated using a relatively simple ray-tracing method. The transport model is segmented into discrete spatial intervals, i.e., a spatial mesh. The mesh interval boundaries are dictated by the spatial variation in the preceding source terms. For each discrete energy gamma, within each mesh interval, for several directions of travel, the line-integral of the photon attenuation coefficient is computed along the ray from the gamma's point of origin to the exterior surface of the model. This ray-tracing procedure calculates the number of uncollided gammas escaping the model's outer boundary.

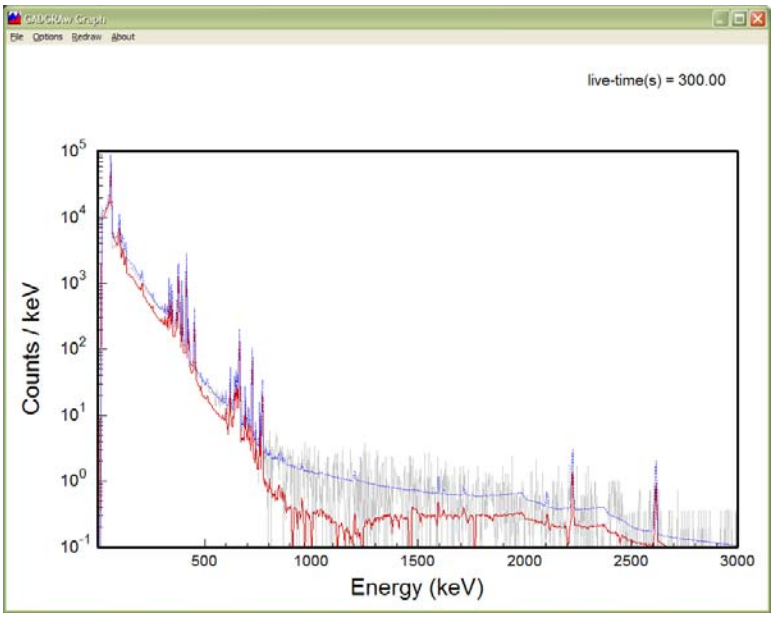

Figure 9. Comparison of old and new transport calculations to measurement of a 2.2-kg weapons-grade plutonium metal sphere reflected by 4.4 cm of polyethylene (measurement shown in gray, old calculation in red, new calculation in blue)

4 GADRAS Integration

The new transport framework has been integrated into the GADRAS graphical user interface, and it is now distributed as a "beta" release that users can unlock. This approach to distribution permits the majority of users to continue to use the old framework while other "beta test" users, primarily internal to Sandia, assist in the continuing testing of the new transport framework.

In the very near future, the new transport framework will be activated by default for all users. The primary differences users will notice include:

- The new framework permits models to be created in one-dimensional spherical, cylindrical, and rectilinear (slab) geometries. The old framework only supports spherical geometries.
- The new framework runs most problems substantially faster than the old framework. This improvement in performance will be most noticeable in the iterative solution of model optimization problems.
- The new framework will permit users to compute the response of the neutron multiplicity counters. In particular, the new framework will compute and display the Feynman-Y.
- There have been several changes and enhancements to the neutron detector response model. Most of these changes enable more accurate computation of the Feynman-Y.

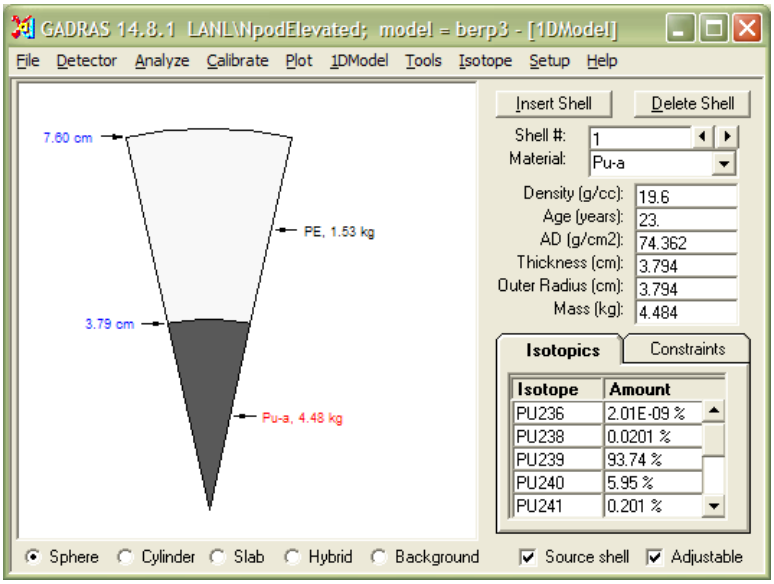

Figure 10. One-dimensional transport model page in GADRAS

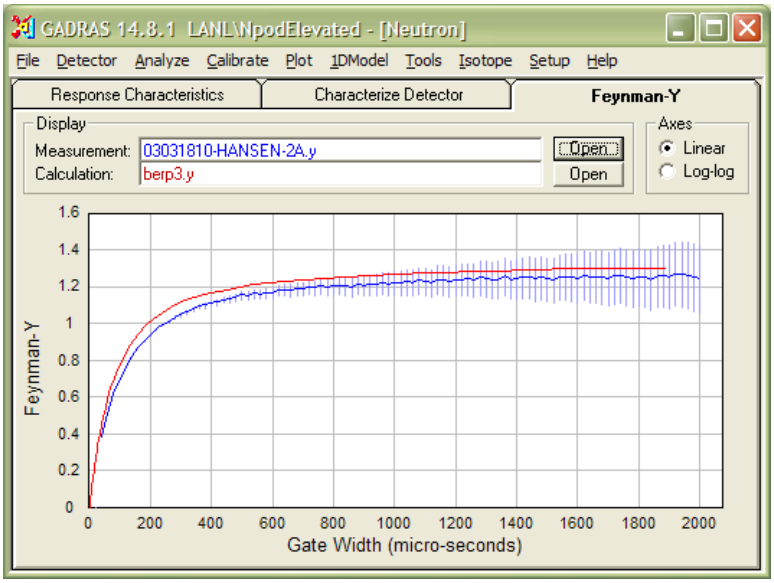

Figure 11. Feynman-Y page in GADRAS

4.1 Neutron Detector Response

The response of a gross neutron counting instrument is computed by integrating the computed neutron leakage current against an energy-dependent detection efficiency. This response model is estimated by unfolding the energy-dependent efficiency from a series of calibration measurements of bare and moderated californium-252.

The response model is characterized by a small number of parameters that primarily estimate the amount of neutron moderation and shielding surrounding the detector's sensing elements. These response model parameters are estimated by searching a

series of pre-calculated detection efficiency curves for the efficiency that most consistently matches all of the californium-252 calibration measurements.

During the development of the new transport framework, the neutron detector response model was extended to include the timing characteristics of neutron multiplicity counters. In addition, areas where the neutron detector response model might be improved were identified.

4.1.1 Neutron Multiplicity Counter Response

Neutron multiplicity counters are generally used to accumulate the number distribution (a.k.a., the multiplicity distribution) of neutron counts as a function of counting time (a.k.a., coincidence gate width), where the counting time generally varies from a few microseconds up to several milliseconds. Consequently, neutron multiplicity counters can be used to characterize both the multiplication of neutrons via induced fission chain-reactions and the dynamic evolution of those chain-reactions.

As described in the preceding neutron transport solver section, the dynamic step response of the system is computed by solving the time-dependent neutron transport equation. In order to correctly model the effect of the detector's dynamics, the solution to the time-dependent transport problem is convolved with the detector's time-dependent impulse response, which is modeled as a simple exponential $e^{-t/\tau}$. The detector time-constant τ reflects the mean neutron slowing-down time in the detector moderator. The time-constant is relatively easy to determine from a single measurement of a spontaneous fission (e.g., californium-252) or (α, n) (e.g., americium-beryllium) source.

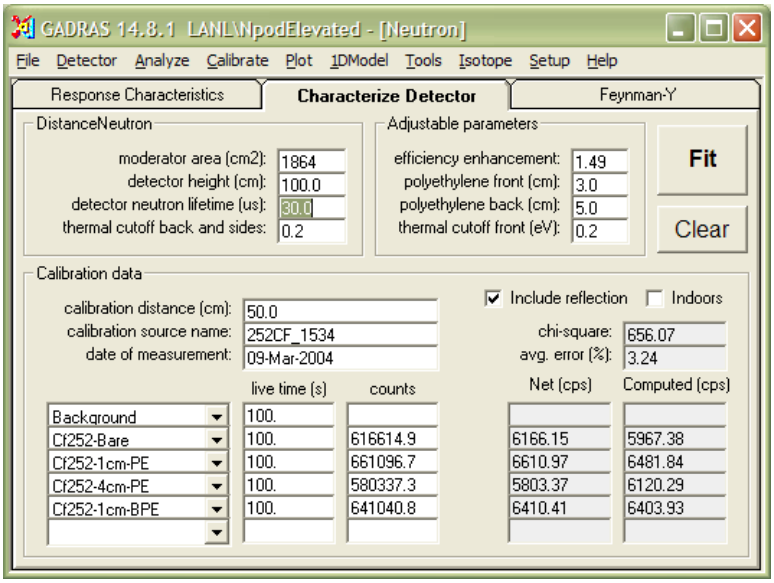

Figure 12. Neutron detector characterization page in GADRAS; neutron time-constant is highlighted on upper-left side

4.1.2 Improvements to Neutron Detector Response Model

4.1.2.1 Neutron detection efficiency

The matrix of detection efficiency curves used to estimate the parameters of the neutron detector response model was calculated using Monte Carlo models of generic arrays of proportional counters embedded in polyethylene moderators. The original calculations used to generate this calibration set were conducted in 1993 using the multi-group Monte Carlo code MORSE, developed at ORNL [Mitchell et al. 1993, Emmett]. The MORSE calculations used the predecessor to the SNAPPLE neutron cross-section library (probably the BUGLE-80 library or some derivative) [Roussin]. Consequently, those calculations use the same coarse group structure at thermal energies, and they do not account for upscatter of highly thermalized neutrons.

As a result, problems have been observed in the accurate calculation of neutron count rates for highly thermalized sources. Those errors were relatively slight, so the source of the problem was not previously identified. However, the coarse thermal group structure and lack of upscatter produced pronounced errors in the computation of the Feynman-Y.

As discussed previously in the section on neutron transport cross-sections, a new neutron cross-section library, Kynea3, was developed to help fix those problems. The Kynea3 library uses a relatively finer thermal group structure, and its scatter matrices contain upscatter elements. Use of the Kynea3 library improved the accuracy of both gross neutron count rate and neutron multiplicity metrics. The library's integration into the transport framework necessitated a new series of detection efficiency calculations.

A new matrix of detection efficiency curves was calculated using MCNP models of the same generic arrays of proportional counters embedded in polyethylene moderators [Harding et al.]. MCNP is a continuous energy code, and it incorporates physical models to correctly estimate the upscatter of thermal neutrons. Consequently, the new detection efficiency curves do not suffer from the same deficiencies as the earlier MORSE calculations. The new models of neutron detection efficiency have been integrated into the GADRAS neutron detector response model, and in general they have improved the accuracy of gross neutron count rate and neutron multiplicity metric calculations.

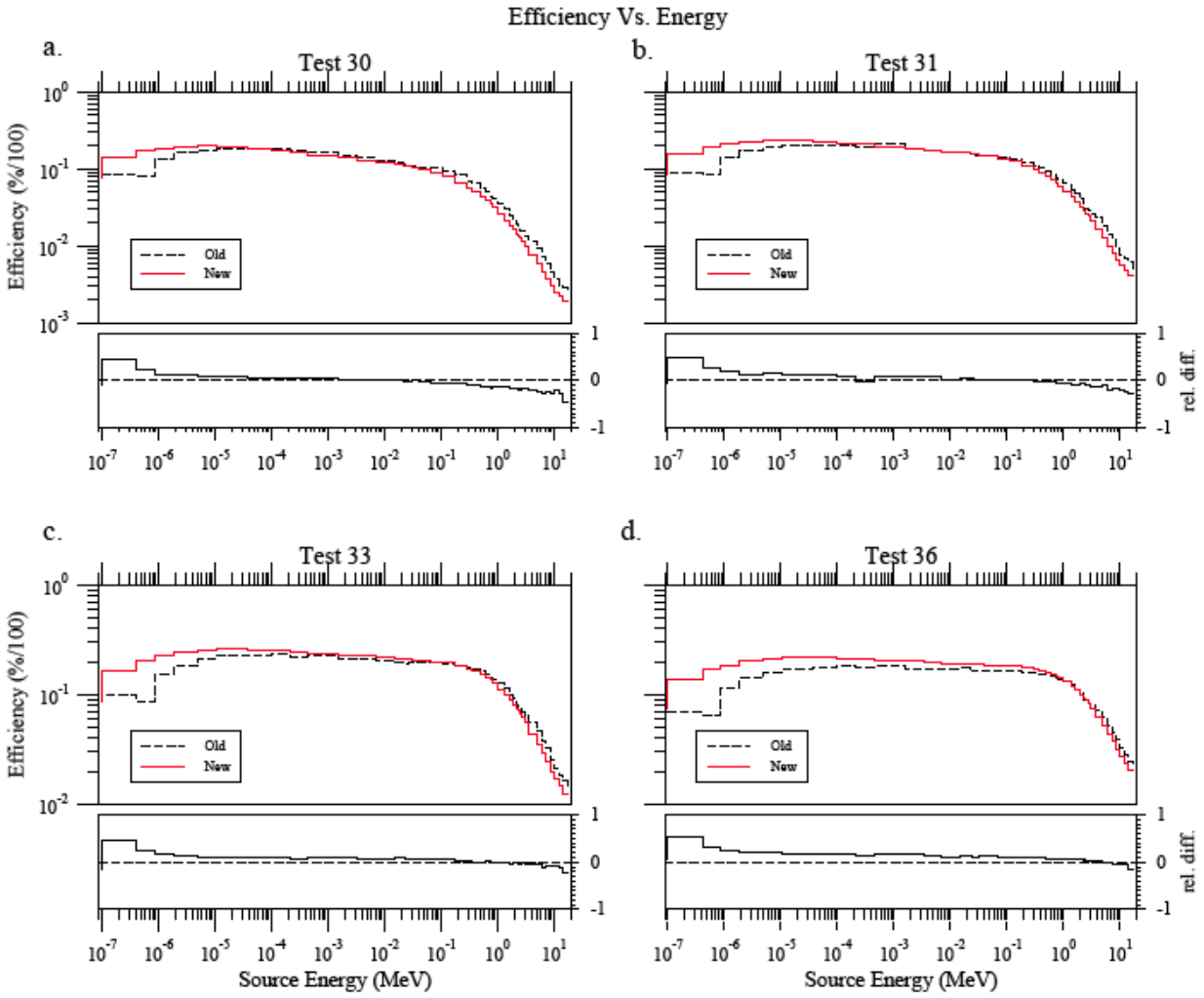

Figure 13. Comparison of old MORSE detection efficiency calculations to new MCNP calculations (MORSE in black, MCNP in red)

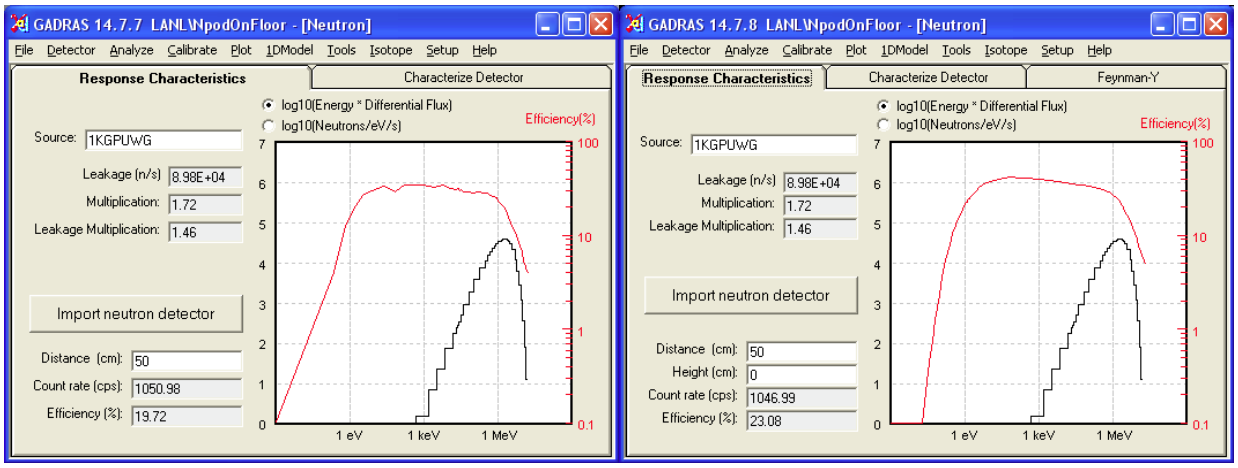

Figure 14. Comparison of old and new neutron response models (old on the left, new on the right)

4.1.2.2 Neutron reflection

Not all detected neutrons travel directly from the outer boundary of the neutron source to the detector. In fact, a substantial portion of the neutrons detected by proportional counters have been reflected back into the detector by the surroundings of the measurement, e.g., the floor. Furthermore, the probability of detecting these reflected neutrons is generally higher than that for their direct, uncollided counterparts, because the scatter interaction(s) involved in neutron reflection tend to slow neutrons down so that they are more likely to be detected.

Prior to 2008, in order to account for neutron reflection, neutron detectors had to be characterized in an environment similar to the environment in which they would be used. Although this approach is reasonable for fixed sensors and for sensors that are rarely moved, it has proven impractical for portable sensors deployed to the field. During 2008 we sought to develop an approximate method to account for neutron reflection that would permit users to adjust the neutron detector response function on demand for the current measurement environment.

Neutron reflection is a three-dimensional effect that can't be exactly modeled in one dimension. However, the principal effect of neutron reflection is to transform the neutron leakage spectrum from one distribution over energy to another distribution over energy. In general, this transformation tends to shift neutrons to lower energies. Consequently, it is possible to approximate the effect of neutron reflection by applying a transformation matrix to the neutron leakage current to estimate the spectrum of reflected neutrons incident on the detector. Alternatively, that same transformation matrix can be used to augment the detector's response for uncollided neutrons to account for its response to reflected neutrons. The two approaches are equivalent; the latter approach was implemented in GADRAS.

The shape and amplitude of the reflection transformation matrix will depend on

- the distance between the source and detector,
- the distance from the source to the reflecting surface (the reflector) and then from the reflector to the detector; and
- the composition of the reflector.

To a first-order approximation, we expect the effect of reflector composition to be dominated by the reflector's hydrogen content, since changes in neutron direction and energy are greatest in interactions with hydrogen.

In order to develop relatively simple models that can be characterized by a handful of parameters, e.g.,

- source/detector distance
- reflector distance; and
- reflector type (e.g., soil, concrete, etc.)

MCNP was used to compute the neutron reflection transformation matrix for varying source-detector and reflector distances. Two reflector materials, soil and concrete, were modeled. These transformation matrices are being integrated into the GADRAS neutron detector response model to permit users to approximately model neutron reflection effects in the field.

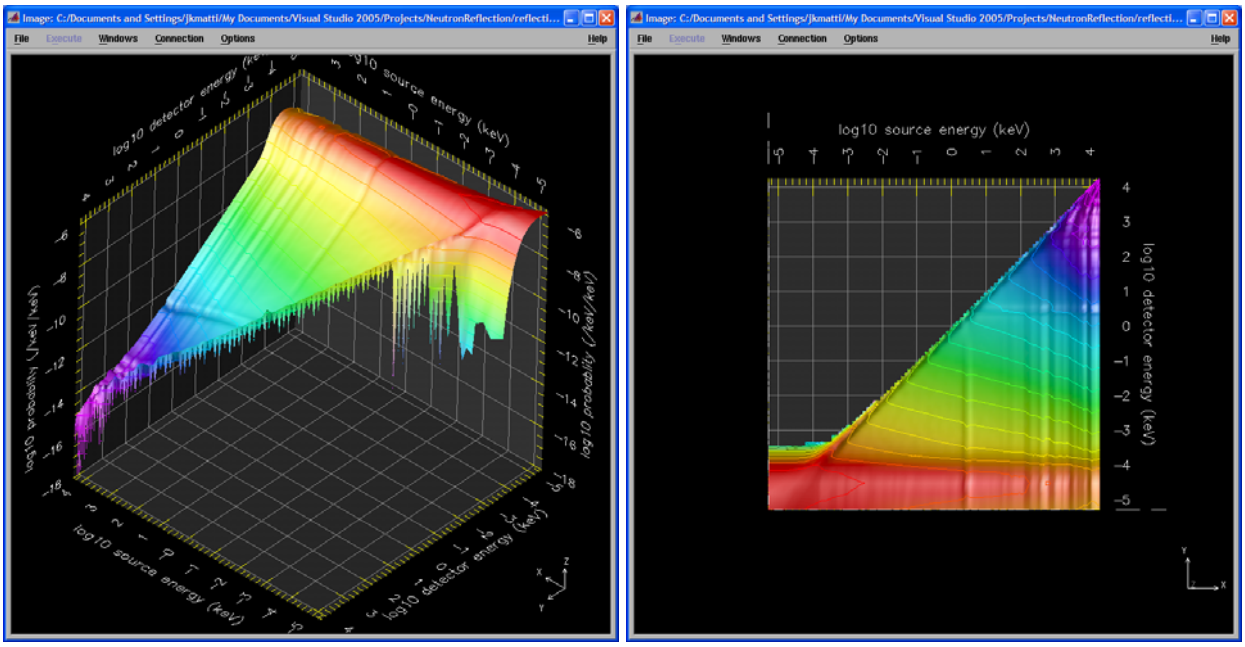

Figure 15. Neutron reflection transformation matrix for the source/detector distance of 1 meter (source and detector both 1 meter above concrete)

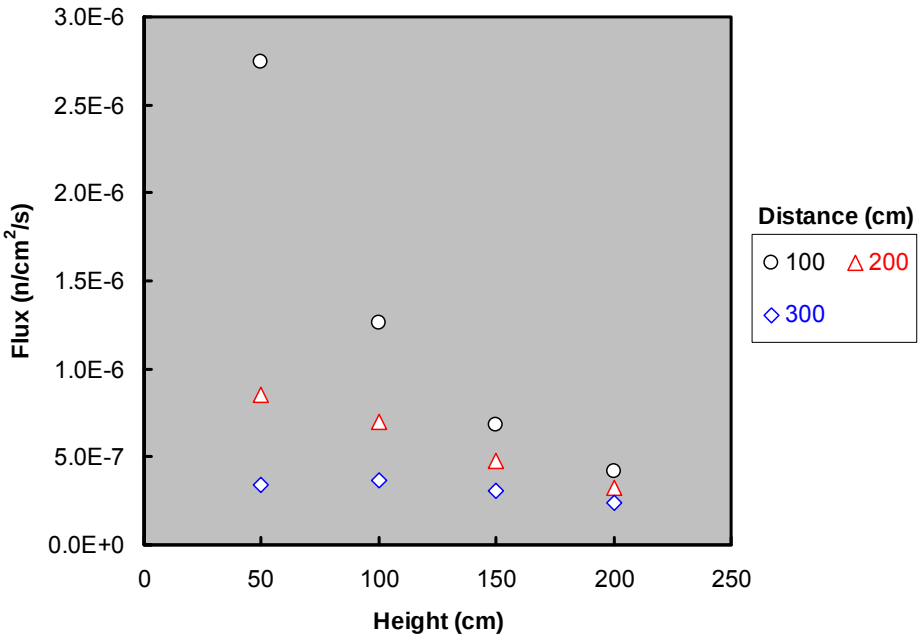

Figure 16. Reflected neutron flux versus source/detector distance and height above concrete reflector

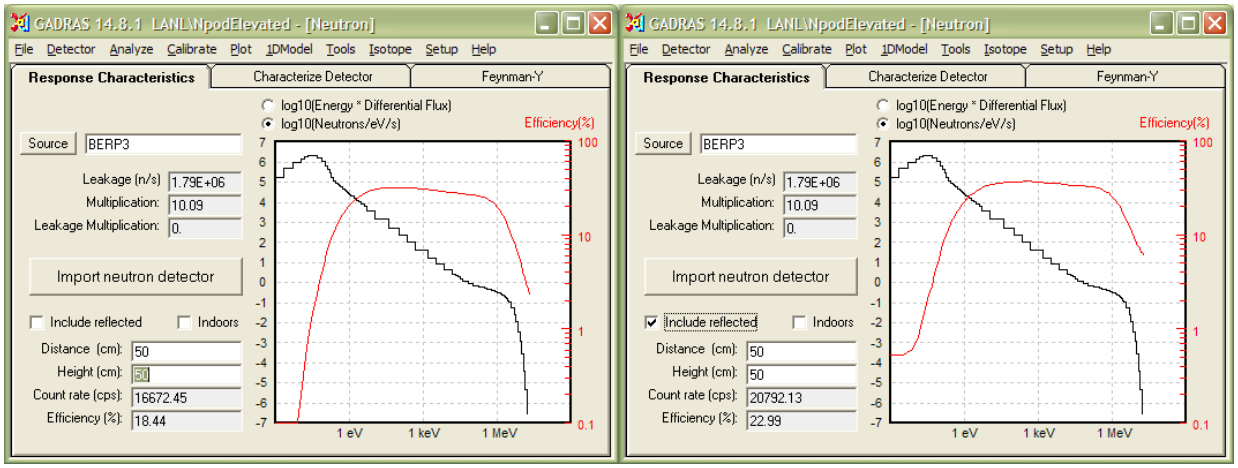

Figure 17. Comparison of neutron detector response model with and without neutron reflection (with reflection on the left, without on the right)

5 Summary

Under the direction of NA-22's SAM program, SNL has developed and tested new radiation transport methods and integrated them into GADRAS. The principal objectives of this project were to

- Develop methods to analyze neutron multiplicity measurements and integrate them into GADRAS.
- Optimize the performance of the GADRAS radiation transport engine.
- Develop and implement improvements to neutron detector response models implemented in GADRAS.

Fast and accurate methods to compute neutron multiplicity metrics using deterministic transport were implemented in GADRAS. These methods enable the solution of inverse transport problems via the simultaneous analysis of gamma spectral and neutron multiplicity measurements. Simultaneous analysis of these two complementary signatures constrains the solution of inverse transport problems more tightly than was previously achievable.

In order to implement the calculation of neutron multiplicity metrics, a new radiation transport framework was developed and integrated into GADRAS. This new framework implements numerous improvements over the original framework. In general, the accuracy of radiation transport calculations in GADRAS has been substantially improved. The speed of these calculations has also improved significantly, which enables inverse transport problems to be solved much more rapidly than was previously possible.

Finally, several improvements have been made to the neutron detector response models implemented in GADRAS. These changes extended GADRAS capabilities to include the modeling of neutron multiplicity counters. They also improved the accuracy of neutron detector response calculations, and they introduced a new capability that permits on-demand modeling of neutron reflection by the measurement environment. Analysts are no longer required to calibrate their neutron detectors in the same environment in which they will be deployed.

This project has substantially extended the capability of GADRAS to support the nonproliferation mission.

References

Adams, K.J., “Electron Upgrade for MCNP4B,” LA-UR-00-3581, Los Alamos National Laboratory, May 2000.

Alcouffe, Ray E. et al., “PARTISN: A Time-Dependent, Parallel Neutral Particle Transport Code System,” LA-UR-05-3925, Los Alamos National Laboratory, May 2005

Alcouffe, Ray E. et al., “DANTSYS: A Diffusion Accelerated Neutral Particle Transport Code System,” LA-12969-M, Los Alamos National Laboratory, June 1995.

Alpan F.A. and M.E. Dunn, “Multigroup Library Generation for Sandia National Laboratory,” Letter Report, Oak Ridge National Laboratory, September 2004.

Cullen, Dermott E., John H. Hubbell, and Lynn Kissel, “EPDL97: the Evaluated Photon Data Library, '97 Version,” UCRL-50400, Vol. 6, Rev. 5. Lawrence Livermore National Laboratory, September 1997.

Emmett, M.B., "MORSE-CGA: A Monte Carlo Radiation Transport Code with Array Geometry Capability," ORNL-6174, Oak Ridge National Laboratory, April 1985

Evaluated Nuclear Structure Data File (ENSDF), http://www.nndc.bnl.gov/ensdf/, Database version of October 16, 2008.

Evans, Robley D. *The Atomic Nucleus*, Krieger Publishing, Malabar Florida, 1955, pp. 548-557.

Firestone Richard B. and L.P. Ekström, *Table of Isotopes*, 8th ed., John Wiley & Sons, 1996. See also http://ie.lbl.gov/toi/, or http://nucleardata.nuclear.lu.se/NuclearData/toi/, accessed October 20, 2008.

Gosnell, Thomas B. and Bertram A. Pohl, “Spectrum synthesis—High-precision, high-accuracy calculation of HPGe pulse-height spectra from thick actinide assemblies,” Lawrence Livermore National Laboratory, November 1999.

Harding, Lee T., John K. Mattingly, and Dean J. Mitchell, “Modernized Neutron Efficiency Calculations for GADRAS,” SAND2008-6073, Sandia National Laboratories, September 2008

Lorence, L.J. Jr., J.E. Morel, G.D. Valdez, “Physics guide to CEPXS: A Multigroup Coupled Electron-Photon Generating Code, Version 1.0,” SAND89-1685, Sandia National Laboratories, October 1989.

Lorence, L.J. Jr., J.E. Morel, G.D. Valdez, “User’s guide to CEPXS/ONEDANT: A One-Dimensional Coupled Electron-Photon Discrete Ordinates Code Package, Version 1.0,” SAND89-1685, Sandia National Laboratories, September 1989

Maienschein, F.C., *Engineering Compendium on Radiation Shielding*, Vol. 1, Springer-Verlag, 1968, 76

Mattingly, John, “Implementation and Testing of Electron Transport in GADRAS,” SAND2005-7785, Sandia National Laboratories, December 2005

Mattingly, John and Eric S. Varley, “Development and Preliminary Testing of Feynman-Y Synthesis in GADRAS,” SAND2007-5427, Sandia National Laboratories, December 2007.

Mitchell, Dean J., Thomas W. Laub, Keith W. Marlow, “Semi-Empirical Response Function for Neutron Detectors,” SAND93-2570, Sandia National Laboratories, October 1993.

Miyasaka, Shun-ichi and Kazuyoshi Minami, “GAMLEG-JR: A Production Code of Multi-group Cross Sections and Energy Absorption Coefficients for Gamma Rays,” JAERI-M 6936, Japanese Atomic Energy Research Institute, February 1977.

Monte Carlo Team, “MCNP – A General Monte Carlo N-Particle Transport Code, Version 5,” LA-UR-03-1987, Los Alamos National Laboratory, October 2005

National Nuclear Data Center, Brookhaven National Laboratory, http://www.nndc.bnl.gov/, accessed October 20, 2008.

Peelle, R.W. and F.C. Maienschein, "The Absolute Spectrum of Photons Emitted in Coincidence with Thermal-Neutron Fission of Uranium-235," USAEC Report ORNL-4457, Oak Ridge National Laboratory, 1970.

Radiation Safety Information Computational Center, http://www-rsicc.ornl.gov/, accessed October 21, 2008/

Roussin, R.W., "BUGLE-80: A Coupled 47-Neutron, 20-Gamma-Ray Group Library for LWR Shielding Calculations," Oak Ridge National Laboratory, June 1980.

SCALE Development Team, “SCALE: A Modular Code System for Performing Standardized Computer Analyses for Licensing Evaluation,” Version 5.1, ORNL/TM-2005/39, November 2006

Terrell, James, "Distributions of Fission Neutron Numbers," *Physical Review* 108(3), 1957, 783.

Valentine, Timothy E., “MCNP-DSP Users Manual,” ORNL/TM-13334/2, Oak Ridge National Laboratory, January 2001.

Valentine, Timothy E., “Polyethylene-Reflected Plutonium Metal Sphere Subcritical Noise Measurements,” SUB-PU-MET-MIXED-001, *International Handbook of Evaluated Criticality Safety Benchmark Experiments,* NEA/NSC/DOC(95)03/I-IX, Organization for Economic Co-operation and Development - Nuclear Energy Agency (OECD-NEA), September 2006.

Varley, Eric S. and John Mattingly, “Corrections to the Evaluated Nuclear Structure Data Files (ENSDF) to Accurately Reproduce Measurements of Special Nuclear Material,” SAND2008-5107, Sandia National Laboratories, August 2008.

Varley, Eric S. and John Mattingly, “Rapid Feynman-Y Synthesis: Kynea3 Cross-Section Library Development,” *Proc. of the American Nuclear Society 2008 Annual Meeting*, June 2008

White, J.E. et al., “VITAMIN-B6: A Fine-Group Cross Section Library Based on ENDF/B-VI for Radiation Transport Applications,” Oak Ridge National Laboratory, December 1996. See also J. E. White, R. Q. Wright, D. T. Ingersoll, R. W. Roussin, N. M. Greene, and R. E. MacFarlane, "VITAMIN-B6: A Fine-Group Cross Section Library Based on ENDF/B-VI for Radiation

Transport Applications," from Proceedings of the International Conference on Nuclear Data for Science and Technology, Gatlinburg, Tennessee, pp. 733-736 (May 1994).

Wilson, W.B. and E.F. Shores, “SOURCES 4C: A Code for Calculating (alpha, n), Spontaneous Fission, and Delayed Neutron Sources and Spectra,” LA-UR-02-1839, Los Alamos National Laboratory, April 2002.

Zucker, M.S. and N.E. Holden, "Energy Dependence of the Neutron Multiplicity $P\nu$ in Fast Neutron-Induced Fission for 235,238U and 239Pu," *Trans. American Nuclear Society* 52, 1986, p. 636

Distribution

1 MS 0782 Eric S. Varley (06418) (electronic file)
1 MS 0791 John Mattingly (06418) (electronic file)
1 MS 0791 Dean J. Mitchell (06418) (electronic file)
1 MS 0791 Lee T. Harding (06418) (electronic file)
1 MS 9406 Nathan R. Hilton (08132) (electronic file)

1 MS 0899 Technical Library, 09536 (electronic file)


Sandia National Laboratories